Competitive Binding of Cd and Zn with the Phytochelatin (γ-Glu-Cys) 4 -Gly: Comparative Study by Mass Spectrometry, Voltammetry-Multivariate Curve Resolution, and Isothermal Titrat...

ARTICLE *in* ENVIRONMENTAL SCIENCE AND TECHNOLOGY · MAY 2008

Impact Factor: 5.33 · DOI: 10.1021/es702725a · Source: PubMed

5 AUTHORS, INCLUDING:

Rafel Prohens
University of Barcelona
49 PUBLICATIONS **737** CITATIONS
SEE PROFILE

José Manuel Díaz-Cruz
University of Barcelona
120 PUBLICATIONS **1,352** CITATIONS
SEE PROFILE

Cristina Ariño
University of Barcelona
102 PUBLICATIONS **1,165** CITATIONS
SEE PROFILE

Miquel Esteban
University of Barcelona
189 PUBLICATIONS **2,459** CITATIONS
SEE PROFILE

Environ. Sci. Technol. **2008,** *42,* 2860–2866

Competitive Binding of Cd and Zn with the Phytochelatin (γ-Glu-Cys)$_4$-Gly: Comparative Study by Mass Spectrometry, Voltammetry-Multivariate Curve Resolution, and Isothermal Titration Calorimetry

ELENA CHEKMENEVA,[†] RAFEL PROHENS,[‡] JOSÉ MANUEL DÍAZ-CRUZ,[†] CRISTINA ARIÑO,[†] AND MIQUEL ESTEBAN*,[†]

Departament de Química Analítica, Facultat de Química and Unitat de Química Fina, Serveis Científico. Tècnics, Universitat de Barcelona Martí i Franquès, 1-11, E - 08028 Barcelona, Spain

Received October 31, 2007. Revised manuscript received January 17, 2008. Accepted January 23, 2008.

The competitive binding of Cd^{2+} and Zn^{2+} by the phytochelatin (γ-Glu-Cys)$_4$-Gly (PC_4) has been examined using several techniques. Electrospray ionization mass spectrometry is used to determine the stoichiometries of the complexes, while voltammetric data analyzed by multivariate curve resolution with alternating least squares allows one to not only trace the displacement induced by Cd^{2+} or Zn^{2+} in the binding of Zn^{2+}or Cd^{2+}, respectively, by PC_4, but also to obtain a complete overview of the processes involved. Isothermal titration calorimetry is used to determine the related binding and thermodynamic parameters. Results obtained via these different techniques are compared and discussed below. The formation of ternary $CdZn(PC_4)$ and $Cd_2Zn(PC_4)$ complexes was observed.

Introduction

Cadmium is one of the most widespread toxic metals. The cellular mechanisms of its toxicity are still not well understood. Cadmium can contribute to the oxidative stress, induce the lipid peroxidation, change the intracellular glutathione levels, and displace metal cofactors from their enzyme binding sites promoting the aberrant reactions. The most important metal cofactors are zinc and copper that are required in redox reactions, stabilize the charge, and contribute to the biocatalysis. However, supraoptimal concentrations of these essential metals are toxic and present the similar metabolism aberration as nonessential toxic metals.

Among the protecting mechanisms of live organisms against the toxic metals is worth mentioning the biosynthesis of phytochelatins (PC_n). PC_n are small cysteine-rich peptides, containing a primary structure (γ-Glu-Cys)$_n$-Gly (n = 2–11), synthesized by eukaryotes for various cellular functions, notably protection against oxidative stress, metal detoxification, and homeostasis (*1, 2*). PC_n are directly synthesized from glutathione (GSH, γ-Glu-Cys-Gly) under the control of the enzyme PC-synthase, which is activated by heavy metals, in particular Cd^{2+} (*3*). Due to their high Cys-content, PC_n bind metal ions by chelation through the -SH. The mechanism is analogous to that exhibited by metallothioneins (MT) in animal and cyanobacterial cells (*4*).

Environmentally relevant levels of heavy metals induce production of PC_n in laboratory cultures of marine algae (*5, 6*) and in coastal waters (*7, 8*). The exposure of the marine diatom *Phaeodactylum tricornutum* to Zn^{2+} and Cd^{2+} showed that variabilities in PC_n and GSH production can be explained, in part, by metal competition for cellular binding sites (*9*). Thus, fundamental studies of the competition between essential metals (as Zn) and toxic metals (as Cd) is of the highest interest for the understanding of many biochemical and environmentally relevant processes as, for instance, metal toxicity to phytoplankton assemblages and phytoremediation.

Several techniques and methods have been used to characterize PC_n and metal−PC_n complexes: X-ray absorption spectroscopies (*10, 11*); ESI-MS (*12*); capillary zone electrophoresis−ESI-MS/MS (*13*); size exclusion chromatography with off-line HPLC and atomic absorption spectrometry determination of PC_n and metals (*14*); some variants of chromatography-inductively coupled plasma-MS (*15, 16*); gel filtration on Sephadex G50 and kinetic measurements of PC_n and sulfide contents (*17*); precolumn derivatization, HPLC and fluorescence detection (*18*); voltammetry (*19, 20*) and voltammetry assisted by chemometrical methods (*21–23*). Isothermal titration calorimetry (ITC) was first applied in our group to study PC_n interactions with metal ions (*24*).

Comprehensive studies of the metal complexes formed by PC_n in solution are still needed, in particular with the simultaneous presence of some metals and binding competition. Of additional interest is the fact that PC_4 is among the most predominant PC_n in natural cell cultures and, thus, the most involved in phytoremediation processes. Here we report our findings on the competitive binding of Zn^{2+} and Cd^{2+} to PC_4, through a comparative study by ESI-MS, electrochemistry via differential pulse polarography with data analysis by multivariate curve resolution using alternating least squares (DPP/MCR-ALS), and ITC.

Experimental Section

Chemicals and Instrumentation. All reagents were of Merck or Sigma/Aldrich analytical grade. Cd^{2+}- and Zn^{2+}-stock solutions, 1.000 (±2) mg L^{-1}, were Titrisol (Merck). The phytochelatin (γ-Glu-Cys)$_4$-Gly (PC_4) trifluoroacetate was provided by DiverDrugs S.L. (Barcelona, Spain), with a purity of 82.8% (HPLC-MS). The impurities are some minor fragments of PC_n without reduced thiol groups, with negligible impact in the complexation. Ultrapure water (Millipore MilliQ Plus 185 system) was used. All solutions used in experiments were previously deoxygenated with nitrogen and subsequently stored in a tightly closed manner to prevent the oxidation of PC_4.

Electrochemical measurements (via differential pulse polarography, DPP) were performed in a 757VA Computrace (Metrohm Herisau, Switzerland) using a static mercury drop electrode (SMDE, drop area 0.6 mm^2), an Ag|AgCl|3 mol L^{-1} KCl reference electrode and a glassy carbon auxiliary electrode. An Orion SA 720 pH-meter was used for pH control. All measurements were carried out using a glass cell at

* Corresponding author phone: (+34) 93 403 91 17; fax: (+34) 93 402 12 33; e-mail: miquelestebanc@ub.edu.
[†] Departament de Química Analytíca.
[‡] Unitat de Química Fina.

10.1021/es702725a CCC: $40.75
Published on Web 03/10/2008

TABLE 1. Metal PC_4 Complexes Observed in ESI-MS Experiments in Ammonium Acetate/Ammonium Hydroxide Buffer at pH 8[a]

solution	$[PC_4]$ titrant	Cd^{2+}: Zn^{2+}: PC_4[b]	complexes ($M_{r,exp}$)
PC_4	10^{-5}		PC_4(1001)
$Cd^{2+} + Zn^{2+}$	10^{-5} PC_4	0.5:0.5:1	$CdZn(PC_4)$ (1179) $Zn(PC_4)$ (1067) $Cd(PC_4)$ (1117) $Zn_2(PC_4)$ (1133)
$Cd^{2+} + Zn^{2+}$	10^{-5} PC_4	1:1:1	$CdZn(PC_4)$ (1179) $Cd_2Zn(PC_4)$ (1289) $Zn(PC_4)$ (1067) $Cd(PC_4)$ (1117) $Cd_2(PC_4)$ (1227)
$Cd^{2+} + Zn^{2+}$	10^{-4} PC_4	1:1:1	$CdZn(PC_4)$ (1179) $Cd_2Zn(PC_4)$ (1289) $Zn(PC_4)$ (1067) $Cd(PC_4)$ (1117) $Cd_2(PC_4)$ (1227) $CdZn_2(PC_4)$ (1243)
Zn^{2+}+ PC_4	10^{-5} Cd(II)	**0.5**:2:1	$Zn(PC_4)$ (1067) $Cd(PC_4)$ (1117) $CdZn(PC_4)$ (1179)
Zn^{2+}+ PC_4	10^{-5} Cd(II)	**1**:2:1	$Zn(PC_4)$ (1067) $Cd(PC_4)$ (1117) $CdZn(PC_4)$ (1179)
Zn^{2+}+ PC_4	10^{-5} Cd(II)	**2**:2:1	$Cd(PC_4)$ (1117) $Cd_2(PC_4)$ (1227) $CdZn(PC_4)$ (1179)
Zn^{2+}+ PC_4	10^{-5} Cd(II)	**4**:2:1	$Cd(PC_4)$ *(1117)* $Cd_2(PC_4)$ (1227)
Cd^{2+} + PC_4	10^{-5} Zn(II)	2: **1**:1	$Cd(PC_4)$ (1117) $Cd_2(PC_4)$ (1227)
Cd^{2+} + PC_4	10^{-5} Zn(II)	2: **2**:1	$Cd(PC_4)$ (1117) $Cd_2(PC_4)$ (1227)
Cd^{2+} + PC_4	10^{-5} Zn(II)	2: **4**:1	$Cd(PC_4)$ (1117) $Cd_2(PC_4)$ (1227) $Zn(PC_4)$ (1067) $Cd_2Zn(PC_4)$ (1289)

[a] The $M_{r,exp}$ is the mass-charge ratio (the components with only one proton were detected in all measurements). [b] Some numbers in this column are shown in bold to note the progressive increase of the Cd^{2+} or Zn^{2+} fraction.

thermostated room temperature (20 °C). DPP measurements parameters were as follows: voltage step 0.006 V, pulse amplitude 0.05 V, pulse time 0.04 s and drop time 1 s. The potential was scanned in cathodic direction between –0.5 V and –1.1 V.

Positive-mode ESI-MS experiments for mixtures containing PC_4 and both metal ions were performed using a Q-TOF Ultima Micromass instrument. The remaining experiments utilized a Waters Micromass ZQ instrument with Waters 2695 Separation Module Alliance. Instrument control was performed using MassLynx software (v.3.5, Micromass Ltd., Manchester, UK).

Calorimetric measurements were carried out with a VP-ITC MicroCal titration calorimeter (MicroCal, Inc. Northampton, MA).

Procedures. In ESI-MS experiments, direct sample injections (50 μL) in pH 8 ammonium acetate/ammonium hydroxide buffer were carried out at a flow rate of 40 mL min^{-1} with a source temperature of 150 °C and desolvation temperature of 250 °C. The applied voltage was fixed at 3.2–3.5 kV, and the cone potential was maintained at 80 V for the Q-TOF Ultima Micromass instrument and 35–40 V for the Waters Micromass ZQ instrument. Mass spectra were collected throughout an m/z range of 450−2500. A 1:9 acetonitrile (HPLC grade): ammonium acetate (5 mmol L^{-1}) mixture was adjusted at pH 8 and used as mobile phase. This ammonium acetate/ammonium hydroxide buffer is suitable for MS due to its volatility. We tried to reproduce the same conditions for all techniques. The attemps to perform MS measurements in TRIS buffer (as in DPP and ITC) failed because of its low volatility. In the present study, competitive binding was analyzed via three different experimental designs: (a) additions of equimolar mixtures containing Cd^{2+} and Zn^{2+} to PC_4 at 10^{-5} mol L^{-1} and 10^{-4} mol L^{-1}; (b) successive additions of Cd^{2+} to a Zn-PC_4 mixture; and (c) successive additions of Zn^{2+} to a Cd−PC_4 mixture.

DPP titrations were performed in 0.02 mol L^{-1} TRIS (pH 7.4)−0.1 mol L^{-1} KNO_3 buffer solutions: 25 mL of a 1×10^{-5} mol L^{-1} PC_4 solution were placed into the cell and purged with pure nitrogen for 40 min. DPP curves were then recorded. After recording reproducible DPP curves of PC_4, aliquots containing 1×10^{-3} mol L^{-1} metal ion solution were added, and the respective DPP curves were recorded, followed by the sequential addition of the second metal ion solution. Experiments involving an equimolar metal ion mixture were performed in both direct and inverse modes: i.e., titration of the PC_4 solution with the metals mixture solution and vice versa. After every addition, solutions were purged with nitrogen and mechanically stirred for 1.5 min.

ITC measurements were carried out at 25 °C as follows: the binary equimolar solution of PC_4 and metal ion (2×10^{-5} mol L^{-1}) was placed in the cell, and the automatic titration with the second metal ion in the syringe (5×10^{-4} mol L^{-1}) was then performed. For a typical experiment, 10 μL of titrant were added to the cell solution, with intervals of 240 s between injections to achieve complete equilibration. The heat of dilution, measured by the injection of titrant to the buffer solution, was subtracted from each titration in order to obtain the net reaction heat value. Metal (Cd^{2+} or Zn^{2+}) and PC_4 solutions were in 0.02 mol L^{-1} TRIS (pH 7.4)−0.1 mol L^{-1} NaCl buffered media.

Data Treatment. *ESI-MS Experiments.* Mass spectra deconvolution was performed by means of MassLynx Software (v.3.5, Micromass Ltd., Manchester, UK).

Electrochemical Experiments. DPP curves were smoothed and baseline-corrected, when necessary, and converted into data matrices using proprietary programs developed by Matlab (*25*). The MCR-ALS method for the analysis of electroanalytical data, summarized elsewhere (*21–23*), are available at http://www.ub.edu/gesq/mcr/mcr.htm.

ITC Experiments. The fitting of ITC data to different binding models by nonlinear least-squares approach (Levenberg–Marquardt algorithm) was done with MicroCal Origin software (*26*). In this study, the one set of sites, sequential binding and competitive binding models were applied. The basic principles of these mathematical approaches are summarized elsewhere (*27, 28*).

Results and Discussion

1. ESI-MS Experiments. Direct-injection ESI-MS is an extremely powerful technique to obtain the stoichiometries of those complexes formed under given conditions at different M:PC_4 ratios. Although ESI-MS experiments for the binary Cd−PC_4 and Zn−PC_4 systems have been previously published (*23*), we studied competitive binding by analyzing samples obtained from three different experimental designs (see the Procedures section). Table 1 summarizes the different metal complexes detected, while Figure S1 in the Supporting Information (SI) shows some representative spectra. The uncomplexed PC_4 presented the well defined signal at $M_{r,exp}$

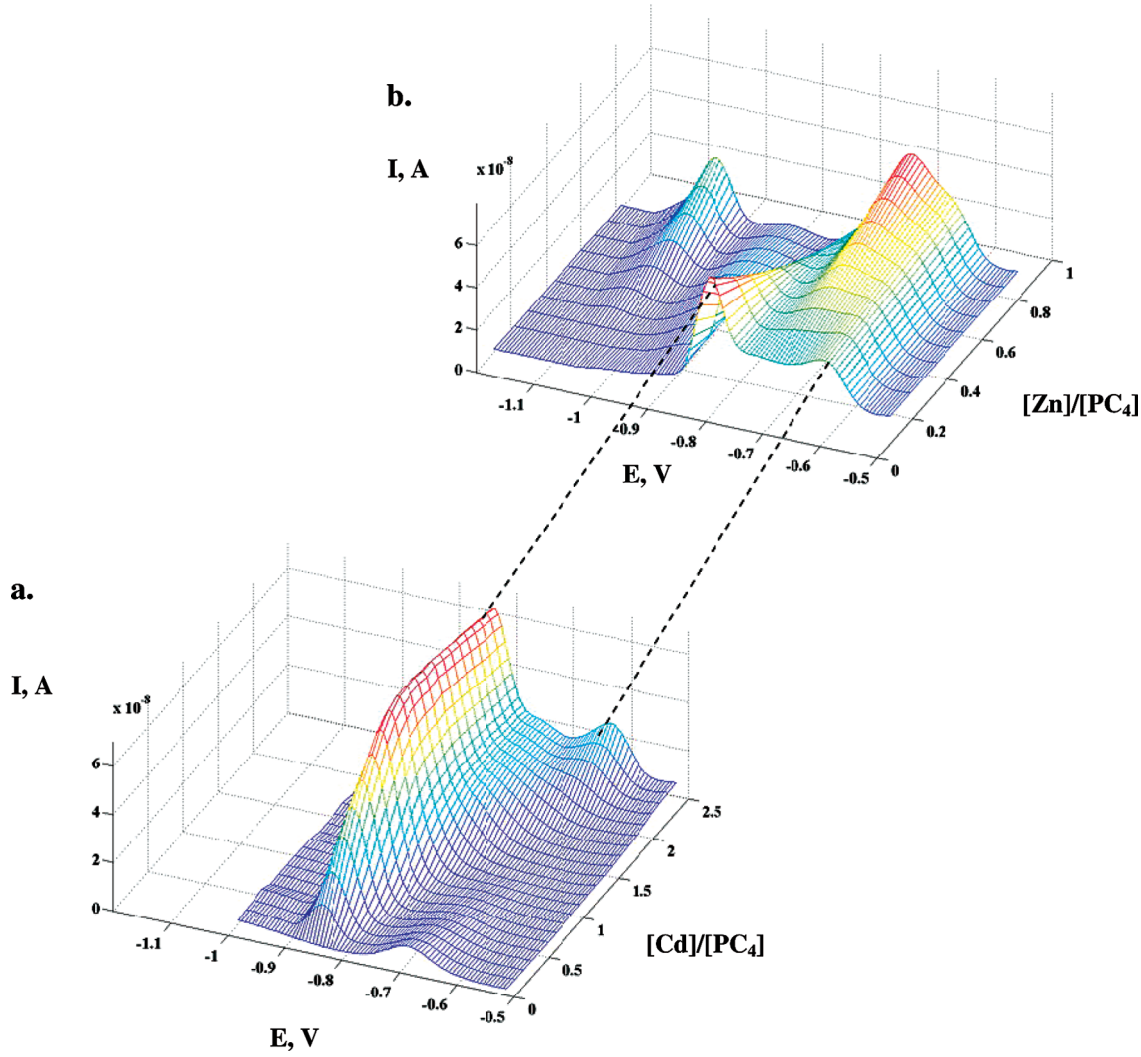

FIGURE 1. DPP curves for the titration of PC_4 with Cd^{2+} in TRIS buffer at pH 7.4 (a) and the following titration of this solution with Zn^{2+} (b). Phytochelatin concentration 1 10^{-5} mol L^{-1}. (Mesh has been plotted from the experimental data matrix after the background current subtraction and the smoothing of individual polarograms).

= 1001 ((PC_4+ H^+)/1). In all the cases, ternary complexes were found. MS signals at 10^{-4} mol L^{-1} PC_4 were more intense (Figure S1c) and exhibited the same complexes as occurred at 10^{-5} mol L^{-1} PC_4, out of $CdZn_2(PC_4)$ ($M_{r,exp}$ = 1243) which was not detected at 10^{-5} mol L^{-1} PC_4.

Our results prove that Cd^{2+} is capable of displacing Zn^{2+}, either completely or partially, depending upon the Cd^{2+}-to-Zn^{2+} ratio, and then forming mixed complexes (to a limited extent), $Cd(PC_4)$ and $Cd_2(PC_4)$, the quantity of the latter increasing as Cd^{2+} increases (Table 1).

It is interesting to compare these results with those obtained for the α- and β-MT domains (*29*). It was found that Cd^{2+} does not remove the Zn^{2+} present in the two domains complexes; in fact, Zn^{2+} is incorporated within the previously formed Cd-domains complexes, thereby resulting in mixed complexes that coexist with them. Thus, either the mixed complexes or the pure Cd^{2+} complexes with α- and β-domains contain a greater proportion of Cd^{2+} than Zn^{2+}, thus confirming the higher affinity of MT-domains toward Cd^{2+}. The same tendency was observed in the present study although in the case of PC_4, Cd^{2+} displaced Zn^{2+} from its complexes, either replacing it or forming the aforementioned mixed complexes, albeit to a lesser extent. This finding substantiates the hypothesis that PC_n and MT play a role in live organisms; i.e., protecting and detoxifying toxic metals. Indeed, it is well-known that Cd^{2+} is more toxic than Zn^{2+}.

2. Voltammetric Experiments. In order to obtain a more dynamic picture of these exchange processes, and taking into account the species detected by ESI-MS, several voltammetric experiments were done. DPP titrations were used, because of the extremely high quality of their data, and analyzed by multivariate curve resolution by alternating least squares (MCR-ALS). This DPP/MCR-ALS approach has proven very useful in prior studies involving PC_3 (*22*), and α- and β-MT domains (*30*). MCR-ALS allows one not only to determine the number of components present in certain solution equilibria, but also to understand their evolution throughout the experiment.

Due to the nature of electrochemical measurements, it is important to note that the concept of a "component" in MCR-ALS refers to the signal emanating from an electrochemical process, and not to a chemical species type, as it typically encountered in spectroscopic data (*21*). For those complexes containing two different electroactive sites (e.g., two metal ions reducing at different potentials), two components (i.e., electrochemical processes) are assotiated with a unique chemical species. These considerations play a key role in further interpretating of MCR-ALS results. To this end, component assignments will be maintained throughout this paper. Four different types of experiments were conducted as described below.

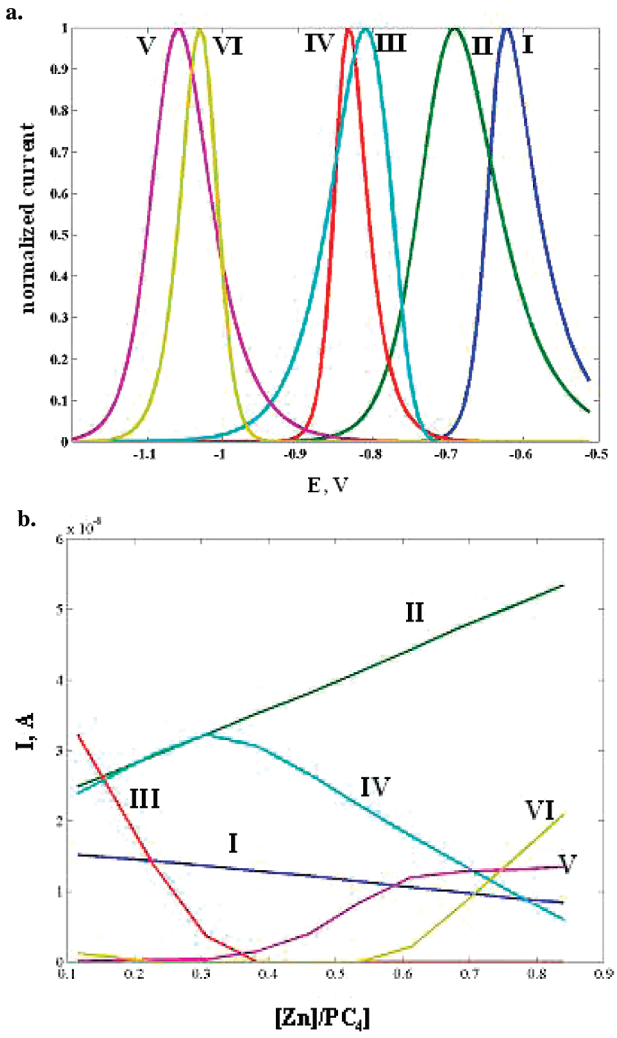

FIGURE 2. Normalized individual voltammograms (a) and concentration profiles (b) obtained from MCR-ALS optimization of the experimental data set from Figure 1b, assuming six components. Constraints: non-negativity for both concentrations and signals, and signal-shape.

2.1. The Addition of Zn^{2+} to the Cd - PC_4 System. This experiment consisted of two steps: (i) an initial titration of PC_4 with Cd^{2+}, until an excess of Cd^{2+} was produced, and then (ii) further titration of the resulting Cd−PC_4 solution with Zn^{2+}. The first step (Figure 1a) confirmed previous results showing the presence of free Cd^{2+} and two different bound Cd^{2+} in the complexes $Cd(PC_4)$ and $Cd_2(PC_4)$ (*23*). In the second step (Figure 1b), the signal related to $Cd(PC_4)$ decreased and then disappeared leaving an excess of Zn^{2+}, with a new peak appearing albeit at lower cathodic potential (ca. –0.7 V). The signal of free Cd^{2+} (at –0.61 V) remained constant while that for free Zn^{2+} appeared at [Zn]:[PC_4] of ca. 0.5.

The singular values decomposition (SVD, see ref *21* for details) of the data set from Figure 1b shows that six components are necessary for satisfactory completion. MCR-ALS decomposed it into the concentration profiles and the normalized individual voltammograms shown (Figure 2), with a lack of fit of 12.30%. These DPP/MCR-ALS results, combined with the ESI-MS experiments, reveals that the addition of Zn^{2+} does not release Cd^{2+} from its thiolate-bound forms, since the free Cd^{2+} reduction signal (component I) remains virtually constant (a very slight decrease in relative terms). On the other hand, any addition of Zn^{2+} induced not only a dramatic decrease in the signal of strongly bound Cd^{2+} in

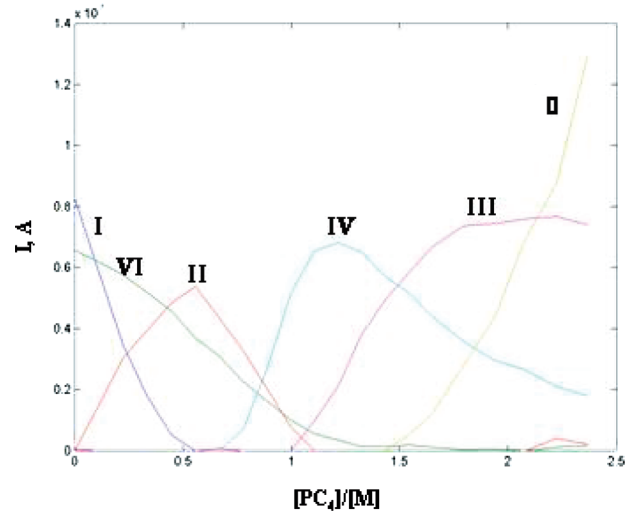

FIGURE 3. Concentration profiles obtained in the MCR-ALS optimization, assuming six components, of the experimental data set from the titration of Zn^{2+} and Cd^{2+} equimolar solution, in TRIS buffer at pH 7.4, with PC_4. Each metal concentration was 1 10^{-5} mol L^{-1}. On the plot [M] refers to Zn^{2+} or Cd^{2+} separately. Constraints: non-negativity for both concentrations and signals, and signal-shape.

$Cd(PC_4)$ (component III), at −0.83 V, but also the increase of component II at a lower cathodic potential (ca. −0.7 V); i.e., a Cd^{2+} bounded less strongly in the ternary Cd−Zn−PC_4 complex.

For satisfactory completion of the system, two components pertaining to Zn^{2+} reduction were required (V and VI), the first (at −1.06 V) assigned to the weakly bound Zn^{2+} by other functional groups of PC_4 (amino or carboxylic) and the second to the free Zn^{2+} reduction at −1.03 V (Figure 2a). Component IV is related to some process that induces the appearance of a low and wide peak at −0.91 V. This signal is not relevant for the exchange process and it seems to correspond to an anodic signal of the Zn−PC_4 complex (*23*). The composition of the ternary Cd−Zn−PC_4 complex related to component II was determined through ESI-MS experiments (Table 1).

Table 2 summarizes the main features of the electrochemical behavior.

2.2. The Addition of Cd^{2+} to the Zn−PC_4 System. The experiment involving the addition of metals in opposite order confirmed the formation of $Zn(PC_4)$ in the first step (*23*), and the capacity of Cd^{2+} to displace Zn^{2+} from its PC_4 complexes in the second step, thus confirming the ESI-MS results. Additional information on this experiment is given in the SI.

2.3. The Addition of PC_4 to an Equimolar Cd^{2+}−Zn^{2+} Solution. As a complementary experiment, an equimolar Cd^{2+}−Zn^{2+} mixture was titrated with PC_4 (see additional information in SI). Its DPP/MCR-ALS analysis, assuming six components deduced from SVD, draws a picture of the process. Figure 3 shows that free Cd^{2+} (component I) is exhausted at a PC_4:Cd ratio of ca. 0.5, when ca. 50% of the initial Zn^{2+} (component VI) is still present in solution. Simultaneously, the signal at −0.7 V (component II) is reaching its plateau, when the concentration ratio of PC_4 to each metal is 0.5. Thus, for 0.5 units of PC_4, 1.0 units of Cd^{2+}, and 0.5 units of Zn^{2+} are complexed. This signal is associated with the reduction of Cd^{2+} bound inside the Cd−Zn−PC_4 complex mentioned above. A $Cd_2Zn(PC_4)$ complex can now be proposed. Inasmuch as PC_4 contains four thiol groups, amino or carboxylic groups are also likely participants in metal binding. With further PC_4 additions, this signal progressively decreases and cathodically shifts upward, with a new peak appearing at −0.83 V that corresponds to a

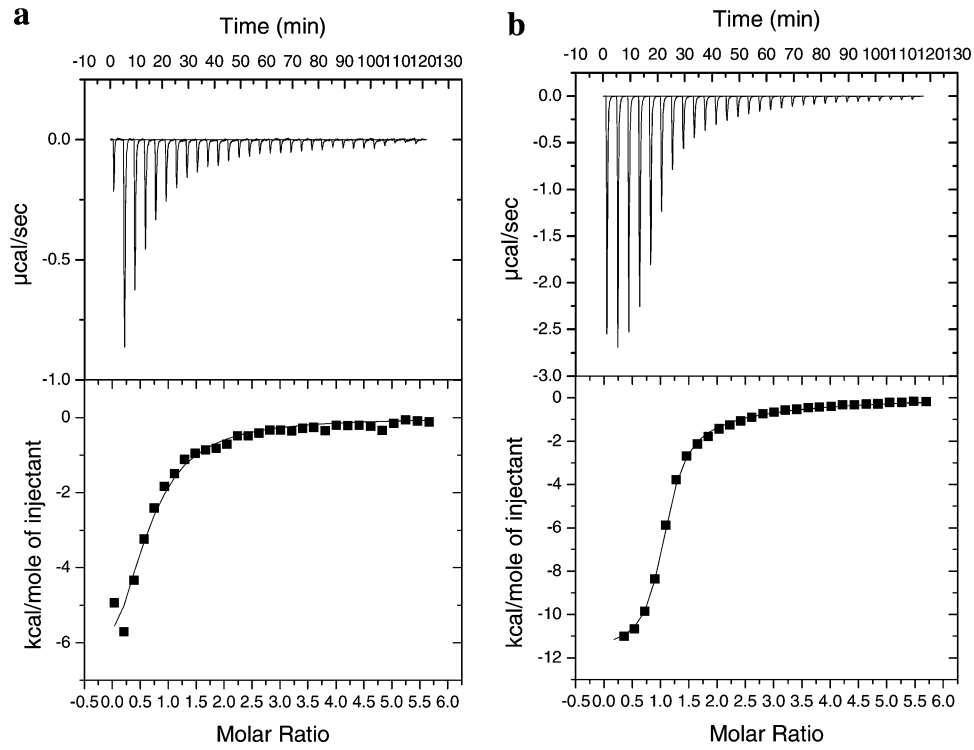

FIGURE 4. Isothermal titration data for the additions of Zn^{2+} to a Cd^{2+}-PC_4 mixture (a) and of Cd^{2+} to a Zn^{2+}−PC_4 mixture (b) in 0.02 mol L^{-1} TRIS (pH 7.4)−0.1 mol L^{-1} NaCl buffered media at 25 °C. Syringe: 5 10^{-4} mol L^{-1} Zn^{2+} (a) or Cd^{2+} (b); calorimetric cell: 2 10^{-5} mol L^{-1} PC_4 and Cd^{2+} or Zn^{2+}. The upper panel shows the calorimetric titrations with 10 μL injections with 240 s time between injections. The lower panel represents the integrated heat values (from the upper panel) as a function of the M^{2+}-to-PC_4 molar ratio in the cell. The solid line represents the best fit to experimental points.

TABLE 2. Components Assignment in DPP/MCR-ALS Experiments[a]

component	potential	electrochemical process	description
0	−0.55 V	$Hg(PC_4) + H^+ \rightarrow Hg^0 + PC_4$	phytochelatin PC_4 signal
I	−0.61 V	$Cd^{2+} \rightarrow Cd(Hg)$	free Cd^{2+} reduction
II	−0.7 V	$Cd_2Zn(PC_4) \rightarrow Cd(Hg) + Zn(PC_4)$	reductions of different Cd^{2+}- complexed forms
III	−0.83 V	$Cd(PC_4) \rightarrow Cd(Hg) + PC_4$	
IV	−0.91 V	$Hg(PC_4) + Zn^{2+} \rightarrow Hg^0 + Zn(PC_4)$	anodic signal
V	−1.06 V	$Zn(PC_4) \rightarrow Zn(Hg) + PC_4$	weakly Zn^{2+}-complexed form
VI	−1.03 V	$Zn^{2+} \rightarrow Zn(Hg)$	free Zn^{2+} reduction

[a] Each component is referred to an electrochemical process, not to a chemical species.

TABLE 3. Thermodynamic Parameters of Competitive Binding in Zn^{2+}−Cd^{2+}−PC_4 Systems in TRIS Buffer (pH 7.4) at 25 °C[a]

titration	site	$K_a \cdot 10^{-5}$, L/mol	ΔH, kcal/mol	ΔS, cal/(mol·K)	fitting model
Zn^{2+} to Cd^{2+}−PC_4	0.61 ± 0.05	2.04 ± 0.50	−7.25 ± 0.80	−0.01	one set of sites
Zn^{2+} to PC_4[b]	0.88 ± 0.02	8.80 ± 0.80	−13.04 ± 0.02	−16.5	one set of sites
Cd^{2+} to Zn^{2+}−PC_4	first	15.30 ± 2.00	−11.47 ± 0.12	−10.2	sequential binding sites
	second	0.20 ± 0.03	−4.58 ± 0.26	4.29	
Cd^{2+} to PC_4[b]	first	42.0 ± 3.5	−16.98 ± 0.10	−26.6	sequential binding sites
	second	0.3 ± 0.03	−5.52 ± 0.26	1.93	

[a] Fitting models: one set of sites and sequential binding sites with two independent binding sites. [b] Data from ref (*24*).

reduction of strongly bound Cd^{2+} in the $Cd(PC_4)$ complex (component III). Since the peak corresponding to free PC_4(component 0, not observed in previous experiments) clearly appears at −0.55 V for $[PC_4]$:[M] > 1.5, this means that for each metal there is ca. one PC_4 molecule. In this case, $[PC_4]$:[M] should be exactly 2. This value was obtained by extrapolating the concentration profile curve at high ratios. Furthermore, this conclusion is consistent with previous studies describing the formation of $Cd(PC_4)$ and $Zn(PC_4)$ complexes (*23*). Upon completing titration, the peak for $Zn(PC_4)$ was not visible due to the electrochemically inert character of this complex inside the studied potential range.

2.4. The Addition of an Equimolar Cd^{2+}−Zn^{2+} Solution to PC_4. The set of voltammograms (not shown) of this titration mode presented a reverse copy of that from the previous experiment (section 2.3). With additions of Zn^{2+}−Cd^{2+}, binary $Cd(PC_4)$ and $Zn(PC_4)$ complexes were initially formed, followed by ternary complexes, and then finally formation of $Cd_2(PC_4)$. Zinc was bound by PC_4 up to an [M]:$[PC_4]$ ratio of 1, while Cd^{2+} remained complexed up to a ratio of 2. The

overall picture of this experiment is consistent with those previously described and confirms that Cd^{2+} is bound more strongly than Zn^{2+}.

Finally, and to confirm that the replacement of Zn^{2+} by Cd^{2+} in PC_4 complexes plays a key role, the complexing capacity curves for PC_4 involving additions of either Zn^{2+}alone or containing a $Zn^{2+}-Cd^{2+}$ mixture were constructed. It was observed that at 1:1 [M]:[PC_4] ratios, variations in free Zn^{2+} reduction peaked faster in the presence of Cd^{2+}, thus confirming the replacement of Zn^{2+} by Cd^{2+} in PC_4 complexes.

Our MS-ESI results are consistent with those obtained by DPP, in which the displacement of Zn^{2+} from its PC_4 complexes was observed following the addition of Cd^{2+}.

3. ITC Experiments. The study on the competitive binding of Zn^{2+} and Cd^{2+} to PC_4 was completed with ITC, which provided useful information regarding the thermodynamic characteristics of these processes. These results can be compared with those of the direct interactions of metal ions with PC_4 monitored by ITC (*24*). Thermograms corresponding to the addition of Zn^{2+} to Cd^{2+}-PC_4, and of Cd^{2+} to $Zn^{2+}-PC_4$, exhibited exothermic patterns (Figure 4).

Thermograms depicting the addition of Zn^{2+} to $Cd^{2+}-PC_4$(Figure 4a) were fitted using the one set of sites model, allowing all parameters to float. The results shown in Table 3 record a fitted stoichiometry value of 0.6, close to the 0.5 value obtained by DPP/MCR-ALS, and a binding constant (K_a) of ca. 10^5 L mol^{-1}. These results demonstrate that Zn^{2+} binds more weakly to $Cd-PC_4$ complexes than to PC_4, as was observed in the direct interaction of Zn^{2+} with PC_4 (*24*). This finding confirms previous results obtained by ESI-MS and DPP/MCR-ALS showing that Zn^{2+} does not displace the Cd^{2+} bound to PC_4, but rather is partially bound to these complexes (*23*). In addition, other functional groups (such as amino or carboxylic) most likely participate in its complexation, thus forming weaker bonds.

In regards to the addition of Cd^{2+} to $Zn^{2+}-PC_4$, previous studies have shown not only that Zn^{2+} is completely displaced from its complexes, but also that two Cd^{2+} are ultimately complexed by PC_4. In this case, it would be appropriate a priori to apply the competitive binding model for the fitting of ITC curves. However, this particular model is limited to those instances in which only two equilibria are present in solution, each of the two ligands (here, Cd^{2+} and Zn^{2+}) interacting with the macromolecule (here, PC_4), and a mixed complex formation is prohibited (*28*). Since the use of other techniques showed the evidence of the mixed complex, a competitive binding model cannot be applied. Table 3 displays the results of ITC curve fitting for the sequential binding sites model for two independent sites with all initial parametres permitted to float.

Thus, we concluded that ITC curves representing the addition of Zn^{2+} to 1:1 Cd:PC_4, in which Cd(PC_4) predominates and Cd_2(PC_4) is of secondary influence, reflect the formation of CdZn(PC_4). Based on the ITC stoichiometric value, which coincided with the electrochemical value, we deduced that only a fraction of Cd(PC_4) was ultimately transformed. When Cd^{2+} additions were made at 1:1 Zn:PC_4 ratio, we observed Zn^{2+} displacement and cadmium complex formations through the intermediate state $Cd-Zn-PC_4$ state.

All the thermodynamic parameters here reported (Table 3) refer to the complex reorganization processes. Comparing these values with those obtained from ITC direct titrations (* data in Table 3), it can be observed that the competitive interaction data are lower, which can be due to the more likely sharing of the thiol groups between Cd^{2+} and Zn^{2+} in the intermediate mixed complex.

In summary, we have here presented results on the competitive binding of Cd^{2+} and Zn^{2+} to the predominant phytochelatin PC_4, which is involved in toxicity processes of phytoplankton species in contaminated stuarine and coastal waters (*9*) and in phytoremediation. As metal-polluted natural systems are typically contaminated by more than one metal, it is helpful to examine the relationships that exist between various metal ions and the metal induced PC_n. The thermodynamic information obtained in this type of studies with PC_n of different sizes can be useful to know the more favorable PC_n for sequestering toxic metals, and thus selecting or modifying the proper plants for phytoremediation studies.

Acknowledgments

We gratefully acknowledge financial support from the Spanish Ministerio de Educación y Ciencia (CTQ2006-14385-C02-01). This research is a part of the activities of SIBA-TEQ group (2005SGR00186) from the Generalitat de Catalunya. E. Chekmeneva acknowledges the University of Barcelona for a Ph.D. grant.

Appendix A

Cys	cysteine
DPP	differential pulse polarography
ESI-MS	electrospray ionization mass spectrometry
Glu	gluthamic acid
Gly	glycine
HPLC	high performance liquid chromatography
ITC	isothermal titration calorimetry
MCR-ALS	multivariate curve resolution with alternating least squares
MS	mass spectrometry
Q-TOF	quadrupole- time of flight
SI	Supporting Information
SVD	singular values decomposition

Supporting Information Available

Additional experimental data concerning ESI-MS experiments (Section 1) and electrochemical studies (Sections 2.2 and 2.3). This material is available free of charge via the Internet at http://pubs.acs.org.

Literature Cited

(1) Callahan, D. L.; Baker, A. J. M.; Kolev, S. D.; Wedd, A. G. Metal ion ligands in hyperaccumulating plants. *J. Biol. Inorg. Chem.* **2006**, *11*, 2–12.
(2) Cobbett, C. S. Phytochelatins and their roles in heavy metal detoxification. *Plant Physiol.* **2000**, *123*, 825–832.
(3) Vatamaniuk, O. K.; Mari, S.; Lu, Y.-P.; Rea, Ph. A. Mechanism of heavy metal ion activation of phytochelatin (PC) synthase. *J. Biol. Chem.* **2000**, *275*, 31451–31459.
(4) Rauser, W. E. Phytochelatins. *Annu. Rev. Biochem.* **1990**, *59*, 61–86.
(5) Ahner, B. A.; Kong, S.; Morel, F. M. M. Phytochelatin production in marine algae. 1. An interspecies comparison. *Limnol. Oceanogr.* **1995**, *40*, 649–657.
(6) Ahner, B. A.; Kong, S.; Morel, F. M. M. Phytochelatin production in marine algae. 2. Induction by various metals. *Limnol. Oceanogr.* **1995**, *40*, 658–665.
(7) Ahner, B. A.; Kong, S.; Morel, F. M. M.; Moffett, J. W. Trace metal control of phytochelatin production in coastal waters. *Limnol. Oceanogr.* **1997**, *42*, 601–608.
(8) Wei, L.; Donat, J. R.; Fones, G.; Ahner, B. A. Interactions between Cd, Cu, and Zn influence particulate phytochelatin concentrations in marine phytoplankton: Laboratory results and preliminary field data. *Environ. Sci. Technol.* **2003**, *37*, 3609–3618.
(9) Kawakami, S. K.; Gledhill, M.; Achterberg, E. P. Effects of metal combinations on the production of phytochelatins and glutathione by the marine diatom Phaeodactylum tricornutum. *BioMetals* **2006**, *19*, 51–60.
(10) Strasdeit, H.; Duhme, A. K.; Kneer, R.; Zenk, M. H.; Hermes, G.; Nolting, H. F. Evidence for discrete $Cd(SCys)_4$ units in cadmium phytochelatin complexes from EXAFS spectroscopy. *J. Chem. Soc. Comm.* **1991**, 1129–1130.
(11) De la Rosa, G.; Peralta-Videa, J. R.; Montes, M.; Parsons, J. G.; Cano-Aguilera, I.; Gardea-Torresday, J. L. Cadmium uptake and translocation in tumbleweed (Salsola kali), a potential Cd-

hyperaccumulator desert plant species: ICP/OES and XAS studies. *Chemosphere* **2004**, *55*, 1159–1168.
(12) McSheehy, S.; Mester, Z. The speciation of natural tissues by electrospray-mass spectrometry. II. Bioinduced ligands and environmental contaminants. *Trends Anal. Chem.* **2003**, *22*, 311–326.
(13) Mounicou, S.; Vacchina, V.; Szpunar, J.; Potin-Gautier, M.; Lobinski, R. Determination of phytochelatins by capillary zone electrophoresis with electrospray tandem mass spectrometry detection (CZE-ES MS/MS). *The Analyst* **2001**, *126*, 624–632.
(14) Scarano, G.; Morelli, E. Characterization of cadmium- and lead-phytochelatin complexes formed in a marine microalga in response to metal exposure. *Biometals* **2002**, *15*, 145–151.
(15) Leopold, I.; Gunther, D.; Neumann, D. Application of high performance liquid chromatography-inductively coupled plasma mass spectrometry to the investigation of phytochelatin complexes and their role in heavy metal detoxification in plants. *Analusis* **1998**, *26*, M28–M32.
(16) Leopold, I.; Gunther, D. Investigation of the binding properties of heavy-metal−peptide complexes in plant cell cultures using HPLC-ICP-MS. *Fresenius' J. Anal. Chem.* **1997**, *359*, 364–370.
(17) Kneer, R.; Zenk, M. H. The formation of Cd−phytochelatin complexes in plant cell cultures. *Phytochemistry* **1997**, *44*, 69–74.
(18) Doring, S.; Korhammer, S.; Oetken, M.; Markert, B. Analysis of phytochelatins in plant matrices by pre-column derivatization, high-performance liquid chromatography and fluorescence-detection. *Fresenius' J. Anal. Chem.* **2000**, *366*, 316–318.
(19) Sestakova, I.; Vodickova, H.; Mader, P. Voltammetric methods for speciation of plant metallothioneins. *Electroanalysis* **1998**, *10*, 764–770.
(20) Scarano, G.; Morelli, E. Determination of phytochelatins by cathodic stripping voltammetry in the presence of copper(II). *Anal. Chim. Acta* **1996**, *319*, 13–18.
(21) Esteban, M.; Ariño, C.; Díaz-Cruz, J. M. Chemometrics for the analysis of voltammetric data. *Trends Anal. Chem* **2006**, *25*, 86–92, and references cited therein.
(22) Cruz, B. H.; Díaz-Cruz, J. M.; Ariño, C.; Esteban, M. Complexation of heavy metals by phytochelatins: Voltammetric study of Cd^{2+} and Zn^{2+} ions by phytochelatin $(\gamma\text{-Glu-Cys})_3\text{-Gly}$ assisted by Multivariate Curve Resolution. *Environ. Sci. Technol.* **2005**, *39*, 778–786.
(23) Chekmeneva, E.; Díaz-Cruz, J. M.; Ariño, C.; Esteban, M. Binding of Cd^{2+} and Zn^{2+} with the phytochelatin $(\gamma\text{-Glu-Cys})_4\text{-Gly}$: a voltammetric study assisted by multivariate curve resolution and electrospray mass spectrometry. *Electroanalysis* **2007**, *19*, 310–317.
(24) Chekmeneva, E.; Prohens, R.; Díaz-Cruz, J. M.; Ariño, C.; Esteban, M. Thermodynamics of Cd^{2+} and Zn^{2+} binding by the phytochelatin $(\gamma\text{-Glu-Cys})_4\text{-Gly}$ and its precursor glutathione. *Anal. Biochem.*, published online Jan 12, http://dx.doi.org/10.1016/j.ab.2008.01.008.
(25) *Matlab version 7.3.0.267*; Mathworks Inc.: Natick, MA, 2006.
(26) *ITC data analysis in Origin®. Tutorial guide. Version 7.0*; MicroCal, LLC: Northampton, MA, 2004.
(27) Jelesarov, I.; Bosshard, H. R. Isothermal titration calorimetry and differential scanning calorimetry as complementary tools to investigate the energetics of biomolecular recognition. *J. Mol. Recognit.* **1999**, *12*, 3–18.
(28) Sigurskjold, B. W. Exact analysis of competition ligand binding by displacement isothermal titration calorimetry. *Anal. Biochem.* **2000**, *277*, 260–266.
(29) Dabrio, M.; Van Vyncht, G.; Bordin, G.; Rodríguez, A. R. Study of complexing properties of the α and β metallothionein domains with cadmium and/or zinc using electrospray ionisation mass spectrometry. *Anal. Chim. Acta* **2001**, *435*, 319–330.
(30) López, M. J.; Ariño, C.; Díaz-Cruz, S.; Díaz-Cruz, J. M.; Tauler, R.; Esteban, M. Voltammetry assisted by multivariate analysis as a tool for speciation of metallothioneins: Competitive complexation of α- and β-metallothionein domains with cadmium and zinc. *Environ. Sci. Technol.* **2003**, *37*, 5609–5616.

ES702725A